

Ground Motion Characteristics in the Chianan Plain of the 2010 Jiasian, Taiwan Earthquake

K. L. Wen^{1,2}, C. T. Chen¹, and J. Y. Huang¹

¹Institute of Geophysics, National Central University, Taiwan

²National Center for Research on Earthquake Engineering, NARL, Taiwan

Abstract

The 2010 Jiasian, Taiwan M_L 6.4 earthquake occurred on March 4, 2010 at 00:18:52 UTC. The epicenter was located in the southern Taiwan (22.969°N 120.707°E) at the depth of 22.6 km. This was the most powerful earthquake in the Kaohsiung area in the recent hundred years. The quake did not cause death, but injured 96 people. Several building was collapsed during the main shock and aftershock. Six trains of THSR (Taiwan High Speed Rail) were disrupted, and one was de-railed while in an emergency braking. This is the first de-railed accident of THSR caused by earthquake in Taiwan. The strong ground shaking also induced the soil liquefaction near the Xinhua town and close to the THSR bridge pier. Fortunately the soil liquefaction only occurred locally did not cause any building damage. In this study, the strong motion data from Jiasian, Taiwan earthquake are analyzed by using the Horizontal-to-Vertical (H/V) spectral ratio method to study the site effect in the Chianan plain. The 2D finite-difference method was used to simulate the wave propagation in the Chianan Plain of the Jiasian earthquake. The results of the simulation demonstrate that the long duration surface wave in the west Chianan plain resulting from the multi-path waves trapped in the top Pleistocene Formation. The simulation can be applied to understanding the strong ground motions expected for future earthquake.

Key word: Jiasian earthquake, Chianan plain, spectral ratio, 2D finite-difference

1. INTRODUCTION

Taiwan is located on the boundary between the Philippine Sea Plate and the Eurasian Plate. The seismicity in the Taiwan is very high. During the 20th century occurred many large and destructive earthquakes close to the Chianan plain. For example $M_L=7.1$ on 1941 December 17, $M_L=7.1$ on 1946 December 5 and $M_L=6.3$ on 1964 January 18. So, southwestern Taiwan has always been considered as probably to occur next big earthquake area. Taiwan is covered with a dense strong motion network array that is operated within the frame of the Taiwan Strong Motion Instrumentation Program (TSMIP) conducted by the Central Weather Bureau (CWB). These recorded events make this study possible to compare with the simulation and the observation. We also use the Horizontal-to-Vertical (H/V) spectral ratio method to conduct the analysis in this study for the Chianan Plain. From the results of the microtremor array research (Lin et al. 2009) and seismic tomography (Wu et al. 2007), we can construct a geometry model to estimate the seismic wave propagations for the area of Chianan plain. In this study we perform 2D Finite-Difference simulations of the Chianan plain for the $M_L = 6.4$ 2010 March 4 Jiasian earthquake. We

analyze the synthetic waveform, peak ground velocity (PGVs), 2 dimension wave propagation snapshots for three 2D profiles. This enables us to understand how the surface wave generated and predicting the ground motions. We expect the results can provide to the future seismic hazard mitigation for the southwestern Taiwan.

2. METHOD

2.1 2010 March 4 Jiasian Earthquake

On 2010 March 4, a $M_L = 6.4$ ($M_w = 5.97$) earthquake occurred near the Jiasian seismic station 17 km to the southeast. This was the most powerful earthquake in the Kaohsiung area since recent hundred years. The intensity reach to 6 and the maximum peak ground acceleration recorded over 460 gal at the CHY062. Shaking map and the stations distribution shown in the Figure 1. The quake caused several building collapsed and one high speed rail train was de-railed. We found near the west part of the Chianan plain excite significant long period and long duration ground motions at periods of about 2-4 sec. The quake was strong enough to trigger about 390 stations of TSMIP network. Therefore, this event provides us enough observations to study the ground motion

characteristic and suitable for comparison of observation and simulation. In this study we simulate 2D wave propagation for three profiles to see how the surface waves generate.

2.2 Horizontal-to-Vertical spectral ratio method

Spectral ratio analysis is a simple method for studying site effects. The spectral ratio from soil and rock station pair was used to analyze the resonance frequency of the soil layer and the amplification factor in traditionally. Choosing a perfect rock station in a wide alluvium plain is difficult. If choose a wrong rock station, such as at mountain of the top or valley, it will be affected by the topography. Nakamura (1989) proposed a single station spectral ratio method, using microtremor data to study the resonance frequency of a shallow soil layer. Field and Jacob (1993) and Lachet and Bard (1994) evaluated this single station spectral ratio method by using theoretical calculation. Lermo and Chávez-García (1993) applied this method to S waves. Because find the perfect reference stations is difficult in this region, we used a single station spectral ratio method in this study. Assuming S_H and S_V are the horizontal spectrum on the surface and the vertical spectrum on the surface. The H/V ratio S_M :

$$S_M = \frac{S_H}{S_V} \quad (1)$$

To take advantage of equation (1), we may realize the site effect in Chianan Plain.

2.3 Chianan Plain Velocity Model

The Chianan plain located in the southern part of the western coastal plain of Taiwan. It's a low, flat and the largest plain in Taiwan. The plain was filled by alluvium deposits, which resulted in flat-lying Quaternary layers. The detail structure of the plain was study by seismic reflection survey (Pan 1967, 1968) and the shallow velocity structure was estimated from surface to a depth of 3 km by the microtremor array measurement (Lin et al. 2009). In this study, we combined the shallow layers velocity and the three main interface's depth (Plio-Pleistocene, Pliocene, and Miocene formations) to create the shallow layer 2D velocity model. We give the S velocity 0.3 km/s and P velocity 1.8 km/s between surface to Plio-Pleistocene interface, Plio-Pleistocene to Pliocene is 0.53 and 2 km/s, Pliocene to Miocene is 1.7 and 3.2 km/s, respectively. Then we embedded the shallow 2D model into the Taiwan area subsurface model by Wu et al. (2007) derived from seismic tomography. Figure 2 display the 2D velocity model used in this study.

Density model is also need for the Finite Difference simulation that is calculated from P wave velocities after Glaznev et al. (1996). The convert equation is given as Eq.(2) and Eq.(3) below :

when V_p less than 5500 m/s:

$$density = 2933 - 518 \times \ln(|vp - 7.595|) \quad (2)$$

when V_p large or equal 5500 m/s:

$$density = 1656 + 1068 \times \ln(|vp - 3.18|) \quad (3)$$

Totally we created four 2D profiles velocity model crossed the epicenter and TSMIP station CHY017, CHY131, CHY021, and CHY023, respectively (Figure 3). Each model has a width 80km and depth 40km.

2.4 Numerical Modeling

We use a 2D Finite-Difference method (Bohlen 2002) for wave propagation simulation. Our simulations are calculated by 4th order standard staggered grid. Damping and one way absorbing boundary (Cerjan et al. 1985) is applied at the left/right, front/back and the bottom to avoid the interference of reflection waves. The calculations are performed on the IBM x3550 supercomputer "Vger" of the center for Computational Geophysics, National Central University. Vger has 108 computing nodes 432 CPUs, calculating performance approach to 3.5TFlops. Our model dimension is 80 × 40 km, grid size is 20 × 20 meters. Therefore, there are 4000 × 2000 = 8,000,000 grids in one model. Estimate Q values model are calculated from the S wave velocity model. $Q_p = 0.1 \times V_s$ and $Q_s = 0.1 \times V_s$, where V_s is in meter/sec. We run the code in the supercomputer use two nodes eight processors for each simulation. Total real time of calculating is about 11 hours. Detail modeling parameters are list in Table 1. We set the source as a double coupling point source. The moment tensor calculated respectively depends on the different azimuth of these profiles. The depth of the source was set to 18 km (BATS) and 22.6 km (CWB). After comparing the waveforms simulated by the different depth. We decide to use the result from the source on depth of 18 km because the result has a better fitting between the observation and the simulation than the result from the depth of 22.6 km

3. RESULTS

3.1 Dominant Frequency

Cutting a 5~10 sec time window of S wave to obtain H/V spectral ratio. After that, the dominant frequency and related amplitude value of the H/V spectrum are picked. The rules of dominant frequency selection were varied from person to person. In this study, the rules are as follows:

1. Choosing the highest of the H/V ratio to be the dominant frequency.
2. If the H/V ratio had the same peak value in the frequency of over two, we may choose the lower one as the dominant frequency.

Figure 4 shows the dominant frequency distribution in the Chianan Plain. The 0.3 to 3 Hz low frequency regions are located near the coastal plain. Most intermediate frequency band of 3 ~ 6.5 Hz are surrounding the basin and the regions near the tableland,

hill, and mountain. Others are high dominant frequency areas, greater than 6.5 Hz. The regions are mainly at the mountain area where the stations are belong to rock site.

3.2 Amplification Effects

Except the dominant frequency can picking from the H/V ratio, it also can be used to understand the spacial variation of the site amplification on different frequency bands. In order to avoid the unusual peak of the H/V ratio, the average H/V ratio in the 1 Hz frequency band were calculated. Figures 5a ~ 5d show the examples of the results for frequency 0.3~1 Hz, 1~2 Hz, 2~4 Hz, and 4~7Hz, respectively. The higher amplification contours areas occurred on deeper alluvium at lower frequency band. At higher frequency band, the higher amplification contours areas occurred shift to near the piedmont. As the frequencies increase, the distributions of higher H/V ratio areas shifted toward the areas of shallow soil.

Figure 6 shows the site amplification at the frequencies of 4~5 Hz, w.r.t. building damage. Damage structures are separated to two kinds by the stories of schools, the white symbols are 1~3 stories, yellow symbols are equal or greater than 4 stories, and the light blue symbols are the stories not known. The stars show the buildings are serious damage and the diamonds are only a little damage.

3.3 Observed and Simulated PGVs

We compare observed and simulated waveforms and peak ground velocity. The observed and the simulated data were all filtered (0.05 Hz-1.0Hz) and rotated to radial and transverse component respectively. We also use 2D to 3D conversion (Miksát et al. 2008) to make the amplitude and waveform correction from 2D simulation. The results of the three stations those nearest to the epicenter CHY061, CHY131 and CHY089 are good fit with the waveform pattern and the peak ground velocity in horizontal component (Figure 7). In general, the vertical component fit is not so good. However, it's difficult to obtain a very good fit in vertical component from simulating. Figure 8 displays observed and simulated velocity waveforms for the stations that far away the epicenter and located on the soft alluvium layer. The PGVs and durations still had a good fit in the horizontal components. The modeling results also show the velocity waveform has a surface wave generated for the station CHY016 and CHY115. Although the pattern of the waveform is not good fit, the 2D simulating still provide us a good way to study the wave propagation and ground motion prediction.

3.4 Wave Fields

Figure 9 display the snapshots of the 2D wave field for the profile CHY131. The snapshots show the waves into a sub Miocene structure (40-50km) during 12-20 sec did not generated the surface wave and caused short

duration. When the waves come into the Pliocene formation the surface wave generated clearly and caused the long duration by the distance increase. Not only the profile CHY131 the other profiles also showed the similar phenomenon. The velocity of the Plio-Pleistocene layer is more slow and soft, but it seems has less influence in our simulation. That is because the Plio-Pleistocene layer is very thin (about 100m) the response of the frequency may be large than 1 Hz. Another reason is our grid size of the model 20 meters is not enough small to analyze such a thin structure. For all this we also found how the surface wave generated very depends on the structure. The surface wave generated almost immediately at the edge of the Pliocene formation for CHY131 and CHY021 model. But this phenomenon did not occur on CHY023 model. The surface wave generated at about 10 kilometers away from the Pliocene formation edge. Figure 10 show the pseudo array radial seismograms of three profiles respectively. The comparing result indicated the shape of the Pliocene interface plays an important role to control the wave propagation and the PGVs value.

3.5 The Event of High Speed Rail Train Derailed

The event of the high speed train, TN#T110, was noticed by public and it is the first case of high speed train derailed due to earthquake in Taiwan. After the sensor received the seismic data, when the ground acceleration is equal or greater than 40 gal, then the alarm system of the Taiwan High Speed Rails will be triggered and started to stop the train. Because we did not have the strong-motion data of high speed rail, we selected four stations which near the alarm station to be as the alarm sensor's station of high speed rail. Based on the time of the high speed rail derailed, it shows the surface wave arrived (Figure 11). Seems the surface wave has some relationship with the train derailed, but it need more study.

4. CONCLUSIONS AND DISCUSSIONS

The schools buildings are serious damage near the epicenter area. Furthermore, the damaged schools are within the areas of high magnification. And the higher stories schools are damaged at the high amplification area of low frequencies in contrast to the lower stories schools are damaged at the high amplification area of higher frequencies. For example, Kaohsiung is an urban area, the most schools are greater than or equal to 4 stories, and the serious damaged schools are located in the high amplification areas of 1-2 Hz.

Assumed the earthquake warning system also installed on the all of strong motion stations it would increase much more time to brake the trains and decrease the probability of derail. After analyzed the waveform from Jiasian earthquake, it might infer that the reason of high speed rail car derailed were due to the surface wave generation.

Our simulations for the Jiasian earthquake on Chianan plain show a good fit with observed and simulated PGVs on radial component. Indicating our numerical modeling is suitable to predicting the ground motions for the area. Even though the vertical simulated PGVs were always overestimate. These may cause by the Q values model are estimated roughly from the V_s . We believe to modulate the attenuate model can solve this and obtain a good fit for vertical PGVs. The snapshots of the wave propagation show the surface wave generated by the shape change of the top layer's interface. The phenomenon also appears in the observation. Unfortunately the observation is not enough along our profile.

We only discuss the velocity waveforms up to 1 Hz in this study. Because we apply a simple velocity model to the top layers. In the further we expect to combine the borehole drilling data and other detail velocity information to create a high resolution velocity model. This may provide us to obtain a higher frequency (up to 3 Hz) of the synthetic waveforms. The result should be a good solution for investigate the wave propagation behavior and predict the ground motion.

Acknowledgements:

We thank Thomas Bohlen for providing 2D Finite-Difference code. We also thank Central Weather Bureau for providing the TSMIP data. The simulations were computed on the "Vger" supercomputer of the center for Computational Geophysics, National Central University. This study is supported by National Science Council, ROC, under the grant no. NSC 98-2116-M-008-008, NSC-99-2116-M-008-023.

References:

- Bohlen, T., (2002), "Parallel 3-D viscoelastic finite-difference seismic modeling," *Computers @ Geosciences*, Vol. **28**, No. 8, 887-889.
- Cerjan, C., Kosloff, D., Kosloff, R., & Reshef, M. (1985), "A nonreflecting boundary condition for discrete acoustic and elastic wave equations," *Geophysics*, **50**, 705-708.
- Field, E.H. and Jacob, K.H. (1993), "The Theoretical Response of Sedimentary Layers to Ambient Seismic Noise," *Geophysical Research Letters*, **20**, 2925-2928.
- Glaznev, V.N., Raevsky, A.B.&Skopenko, G.B., (1996), "A three-dimensional integrated density and thermal model of the Fennoscandian lithosphere," *Tectonophysics*, **258**, 15-33
- Lachet, C. and Bard, P.Y. (1994), "Numerical and Theoretical Investigations on the Possibilities and Limitations of Nakamura's Technique," *J. Phys. Earth*, **42**, 377-397.
- Lermo, J. and Chávez-García, F.J. (1993), "Site Effect Evaluation Using Spectral Ratios With Only One Station," *Bull. Seism. Soc. Am.*, **83**, 1574-1594.
- Lin, C. M., T. M. Chang, Y. C. Huang, H. J. Chiang, C. H. Kuo, and K. L. Wen* (2009), "Shallow S-wave velocity structures in the western coastal plain of Taiwan," *Terr. Atmos. Ocean Sci.*, **22**, 2, 299-308. doi: 10.3319/TAO.2007.12.10.01(T).
- Nakamura, Y. (1989), "A Method for Dynamic Characteristics Estimation of Subsurface Using Microtremor on The Ground Surface," *QR of RTRI*, **30** (1).
- Pan, Y. S., (1967), "Interpretation and seismic coordination of the Bouguer gravity anomalies over west-central Taiwan,"

- Petrol. Geol. Tai wan*, **5**, 99-115.
- Pan, Y. S., (1968), "Interpretation and seismic coordination of the Bouguer gravity anomalies obtained in south western Taiwan," *Petrol. Geol. Tai wan*, **6**, 197-208.
- Miksat J., Müller T. M. and Wenzel F., (2008), "Simulating three-dimensional seismograms in 2.5-dimensional structures by combining two-dimensional finite difference modelling and ray tracing," *Geophys. J. Int.*, **174**, 309-315, doi: 10.1111/j.1365-246X.2008.03800.x
- Wu, Y. M., C. H. Chang, L. Zhao, J. B. H. Shyu, Y. G. Chen, K. Sieh, and J. P. Avouac (2007), "Seismic tomography of Taiwan: Improved constraints from a dense network of strong-motion stations," *Journal of Geophysical Research*, **112**, B08312, doi:10.1029/2007JB004983.

Table 1 Modeling parameters

Parameter	value
Horizontal grid size (m)	20
Vertical grid size (m)	20
Horizontal Dimension (km)	80
Vertical Dimension (km)	80
Number of grid points (H)	4000
Number of grid points (V)	2000
Number of time steps	140000
Simulation time (sec)	140

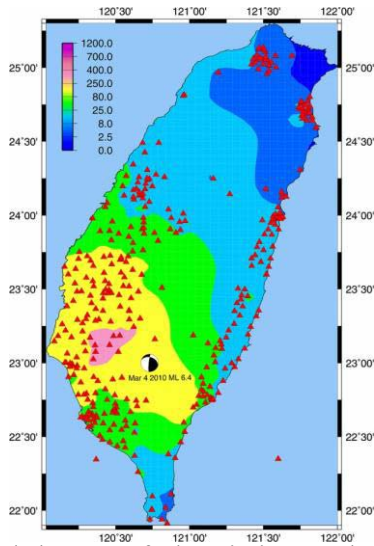


Figure 1 Shakemap of the Jiasian earthquake. Red triangles are the TSMIP stations.

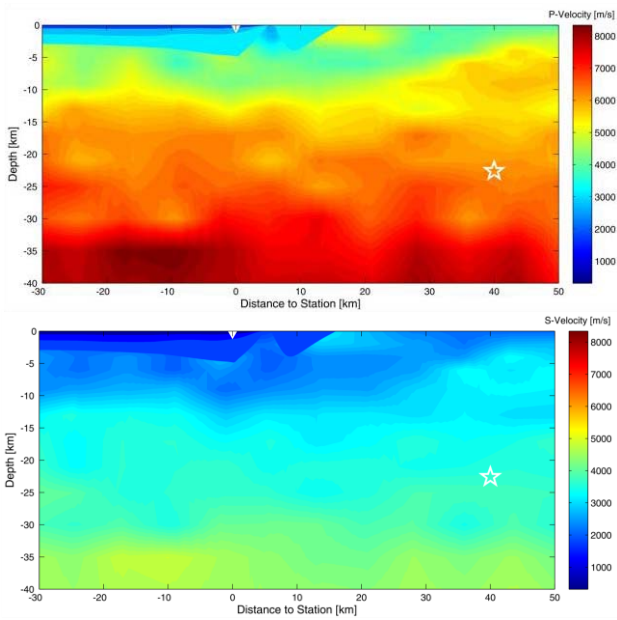


Figure 2 P wave and S wave velocity model. Dimension is 80 km in width 40 km in depth. White triangle is the CHY131 location, star is the source location.

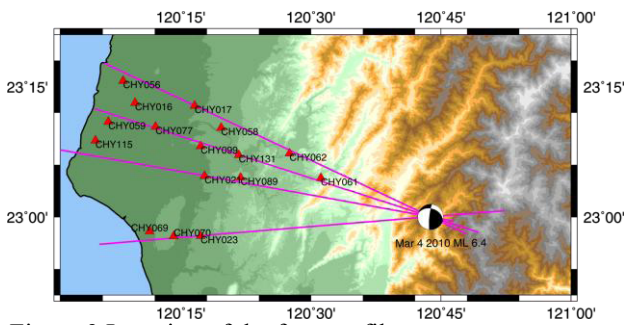


Figure 3 Location of the four profiles.

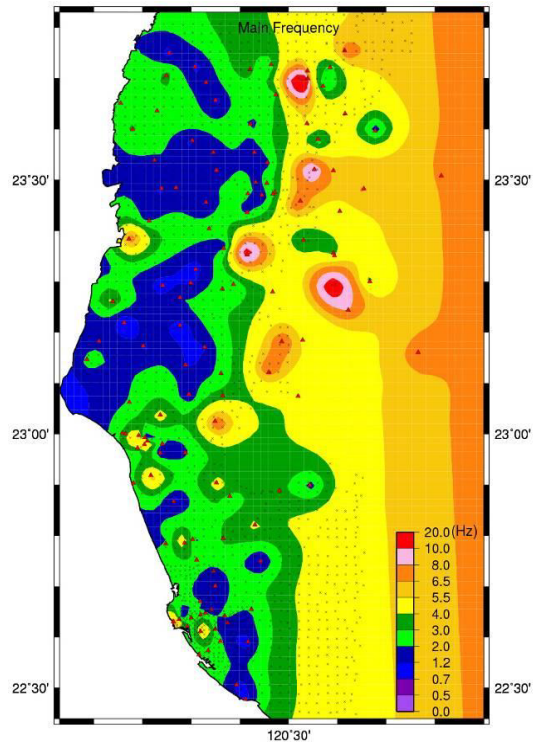


Figure 4 The dominant frequency distribution in Chianan Plain. The red triangles represent the free-field strong-motion stations.

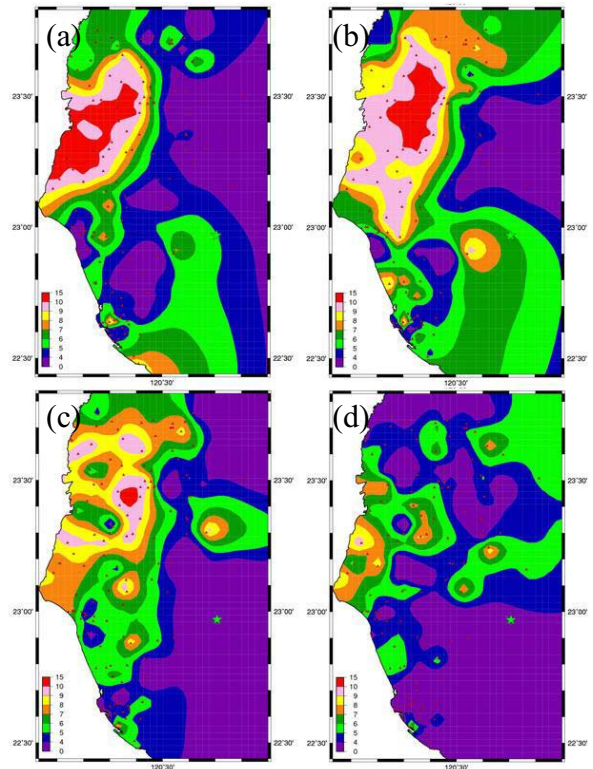


Figure 5 The distribution of site amplification factor. (a) 0.3~1 Hz (b) 1~2 Hz (c) 2~4 Hz (d) 4~7 Hz. The green star is the location of epicenter.

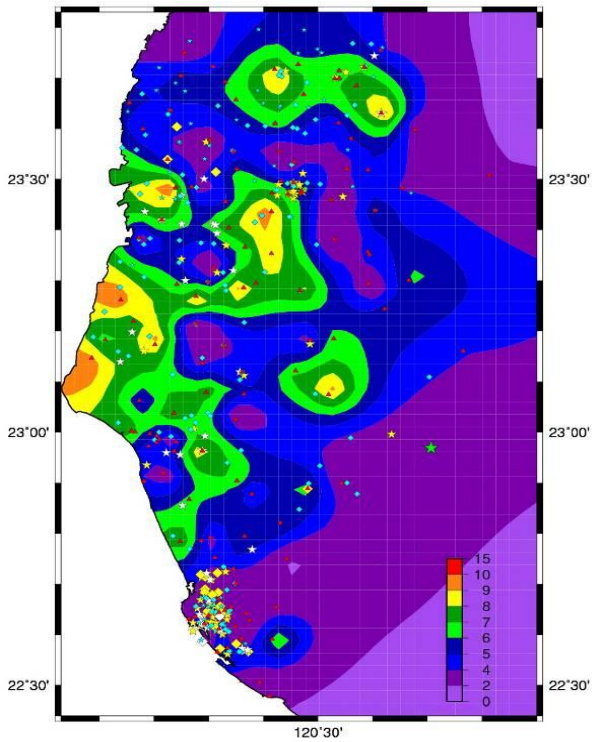


Figure 6 Relationship between dominant frequency and the damaged building's floor. The site amplification is for the frequencies of 4~5 Hz. The green star is the location of epicenter.

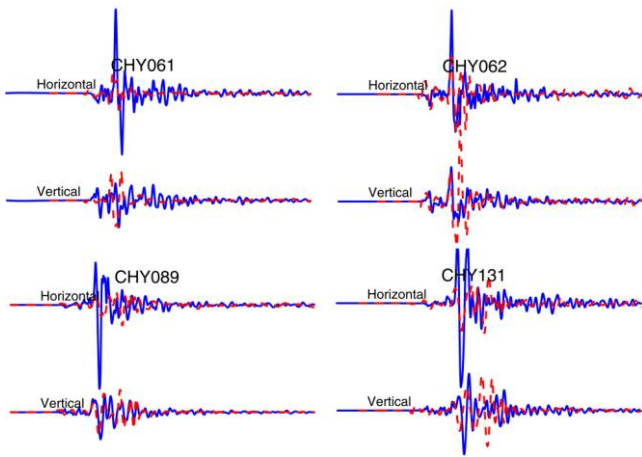


Figure 7 Comparison between observed and simulated velocity waveforms for three stations nearest to the epicenter, duration is 70 sec.

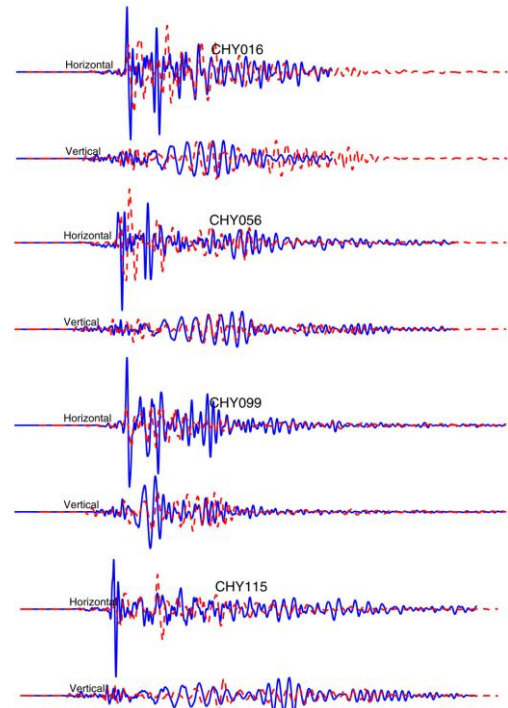


Figure 8 Comparison between observed and simulated velocity waveforms for other stations, duration is 140 sec.

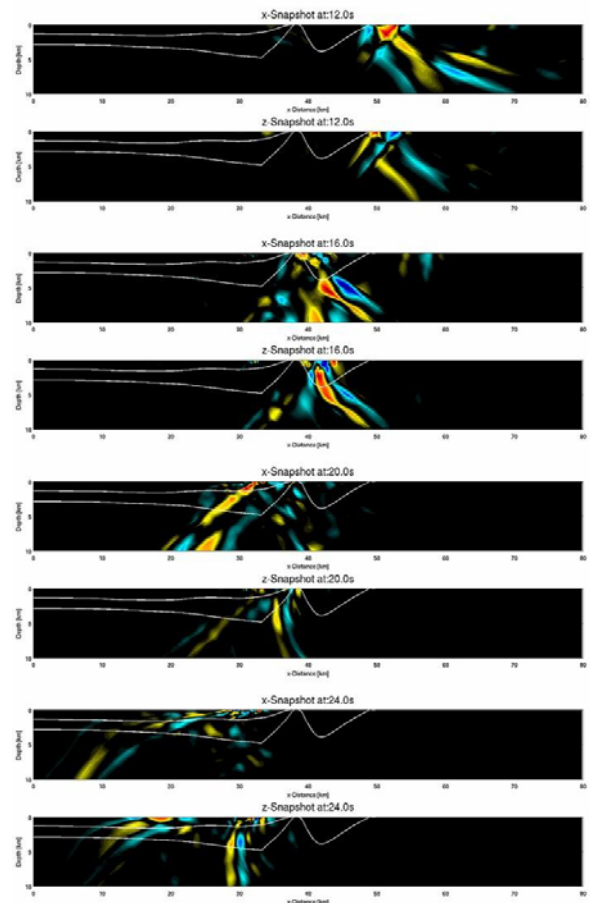


Figure 9 Profile CHY131 snapshots of the radial and vertical components of the simulated velocity wavefield for 12-24 sec. The color map scaled to the maximum velocity.

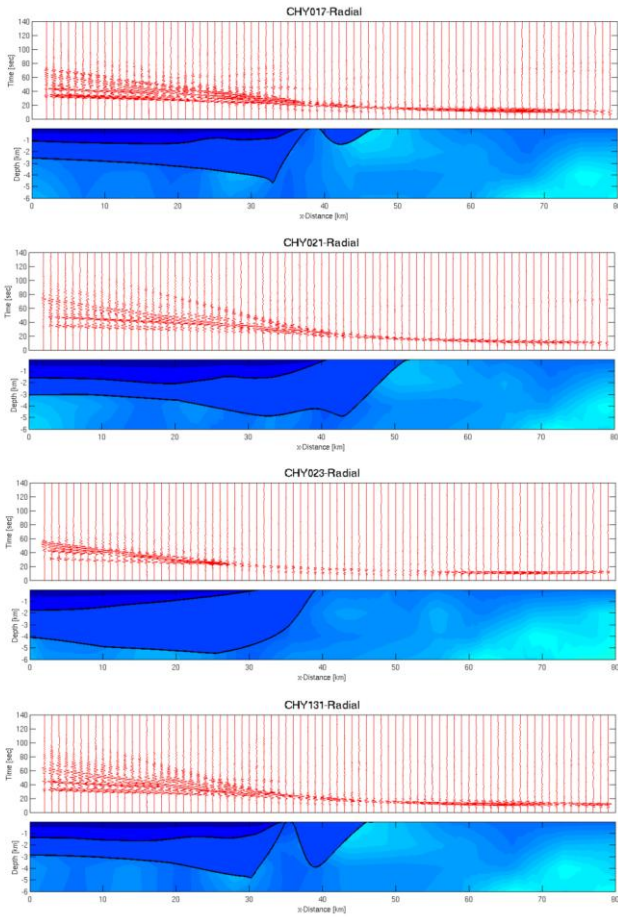


Figure 10 Synthetic pseudo array radial seismograms along four profiles. Top first black line is the interface of the Pliocene formation; second black line is the Miocene interface.

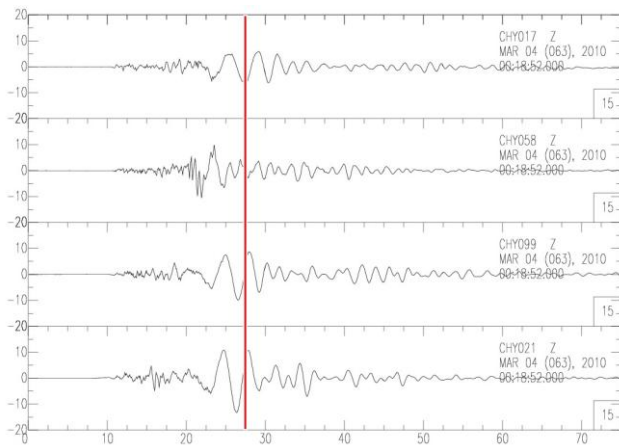


Figure 11 Four velocity waveforms recorded at strong motion station that near the high speed rail. Red line indicates the train derailed time.